TuijinJishu/Journal of Propulsion Technology
ISSN: 1001-4055
Vol. 44 No.6 (2023),

Exploration of Engine Performance on Thermal Barrier Coating Powered by Biodiesel with Al_2o_3 Nanoadditive.

S. Venkateswarlu 2. Dr. P. Balashanmugam 3. Dr. B . Omprakash

[1]*Assistant. Professor, Mechanical Engineering Dept, JNTUACEA, Ananthapuramu pin code 515002.*

[2]*Associate. Professor, Mechanical Engineering Dept,*

Annamalai University, Chidambaram, Tamil Nadu, pin code: 608002.

[3]*Assistant. Professor, Mechanical Engineering Dept, JNTUACEA,*

Ananthapuramu pin code: 515002.

***Abstract*:**

This present examination aims for increasing engine performance by using calibnum inhoblum methyl ester 20% and 80% diesel @ 25 ppm [B20 + 25 ppm of Al_2O_3] nanoparticle additive for the low heat rejection (LHR) engine. The piston crown coating involved a two-layer insulation process. Initially, a 50 µm thick bond coat of Ni-Cr-Al-Y was applied, followed by a topcoat using two different pistons, namely 2% Nd + YSZ (5% yttrium + 2% neodymium oxide + 93% zirconium oxide) and 2% Gd + YSZ (5% yttrium + 2% gadolinium oxide + 93% zirconium oxide), with a thickness of 250 µm. This coating was applied using the plasma spray coating method. In comparison to diesel, the engine performance with B20 + 25 ppm Al_2O_3 resulted in enhancement in brake thermal efficiency (BTE) of 9.7% and a diminish in brake specific fuel consumption (BSFC) of 23.07%. The CO, HC and smoke values were reduced by 24.6%, 38.25% and 11.3%, respectively, compared with diesel fuel. The NOx and EGT were increased by 30.45% and 24.2%, respectively, with full load at 1500 rpm.

Key words: *Thermal Barrier, Biodiesel, Al_2O_3, Nano*

1. Introduction

The increasing demand for power and the concern over pollutants have led to a growing focus on exploring alternative fuel sources that are becoming more readily available with each passing day. The utilization of oil-based products in internal combustion engines leads to a range of environmental problems. Biodiesel, a fuel derived from vegetable oils through specific catalysts, is a response to the pressing challenges encountered by many countries. Scientists have opted for biodiesel and bio-fuels due to their sustainable, viable, and eco-friendly characteristics. To facilitate the commercial production of sustainable biodiesel and bio-fuels, it is crucial to explore the benefits of using non-edible, marginal oil resources to reduce the production costs of these fuels [1].

Numerous scientists have made systematic endeavors to employ unprocessed vegetable oils as a substitute fuel in CI engines. This approach serves to reduce the dependency on non-renewable energy sources and decrease emissions. Unprocessed vegetable oils hold significant value and potential as an eco-friendly alternative to fossil fuels due to their clean and environmentally friendly nature. These unrefined vegetable oils possess a lower flash point, high viscosity, and are known for issues related to auto-oxidation, gum formation, and reduced engine durability at the lower end. When used in the engine without any direct modifications, such oils can lead to damage to engine components and result in notably subpar performance.

Biodiesel shares properties with regular diesel fuel. In both cases, biodiesel exhibits characteristics such as increased density and viscosity, elevated brake-specific fuel consumption (BSFC), and higher levels of smoke emissions [2].

In this study, lemongrass oil was used as a biofuel in varying proportions, including 10%, 20%, 30%, 40%, and 100%, in combination with diesel blends. The B20 blend, which contains 20% lemongrass oil, stands out due to its lower viscosity and improved combustion. Nonetheless, its BTE is marginally lower at 10.07%, which can be attributed to the oxygen element in the fuels and their more cetane number. When comparing it to pure diesel, the B20 blend results in a reduction of 15.37% in HC emissions, 9.21% in smoke opacity, and 6.2% in CO emissions. This reduction is owing to the existence of sufficient oxygen for a more complete combustion and faster consumption during the combustion process. However, the B20 blend does show an 8.3% increase in NOx emissions equated with the base engine, which can be attributed to the elevated temperatures generated during combustion and the greater latent heat of vaporization [3].

In study on fish oil is utilized as a fuel and mixed with diesel in proportions of 20% and 40%. The B20 blends demonstrate an 8.3% improvement in brake thermal efficiency compared to pure diesel. This enhancement is credited to the effective air-fuel mixture and proper combustion. However, the B40 blends exhibit a significant 12.51% improved in NOx emissions equated to diesel. This results from the existence of oxygen within biodiesel, leading to its effective combustion process. On a positive note, carbon monoxide levels are reduced by 33.84% in the B20 blend equated to conventional standard fuel, thanks to the appropriate air-fuel mixture during the combustion process [4-5].

Numerous research studies are currently focusing on the integration of nanoparticles in water emulsions to mitigate pollutant characteristics and improved performance in engines. This study specifically examined the use of nanoparticles (Al_2O_3, CNT, SiO_2) at dosages of 25, 50, and 100 Ppm in conjunction with pure diesel fuels under varying load conditions. The results indicated an impressive 18.8% improvement in BTE [6]. Concurrently, there was a 19.8% reduction in BSFC, mainly attributed to the increased cetane number and the inclusion of oxygen in the fuel. Blends with silicon oxide and alumina exhibited elevated combustion pressures (8.5% and 3.25%, respectively) and a notable 1.76-fold reduction in CO emissions, albeit with negative consequences on NO_X. Conversely, the carbon nanotube blend led to a 4.48% overall increase in NOx emissions, along with higher CO, CO_2, and HC emissions. This is owing to the more oxygen element in nanoparticles, resulting in a more rapid combustion of fuel [7].

The research delved into the influence of incorporating carbon and alumina nanoparticles into diesel-biodiesel blends, contrasting the results with three different fuel variants: diesel-biodiesel blends (B10), B10 with a 4% emulsifier (E), and B10 with 4% emulsifier in combination with 30 ppm nanoparticles (B10E4N30). The findings unveiled that the inclusion of nanoparticle blends led to a significant 6% reduction in BSFC, accompanied by noteworthy decreases of approximately 7% in NO_X emissions and 19% in CO emissions. These improvements are attributed to the appropriate mixing of air and fuel components and a shortened ignition period [8].

Biodiesel water emulsions were enriched with zirconium nanoparticles at concentrations of 50 ppm and 100 ppm. The study revealed that the addition of 100 ppm nanoparticles, when mixed with water, resulted in a 13.25% increase in NO_X emissions equated to pure diesel fuel. This increase can be credited to the moisture content in the fuel, which may limit the combustion duration. However, the pollutant of CO, HC, and smoke visibility decreased significantly by 31.5%, 26.8%, and 14%, respectively, when using the biodiesel water nano-emulsion compared to the biodiesel water emulsion. This reduction is owing to the presence of oxygen in the mixture, which helps in minimizing tailpipe pollutants [9].

Energy consumption is a critical parameter for evaluating internal combustion engines (IC engines). Specifically, the second law of thermodynamics underscores that it is impossible to convert the entire input energy into productive work. Put differently, achieving 100% efficiency is unattainable because there will always be a portion of energy lost as heat in exhaust gases, dissipated as heat loss through the cooling system, and other unaccounted for losses. Over the past few decades, there has been a significant focus on minimizing energy losses to the coolant during power strokes in order to enhance efficiency. Today, there is a growing effort to improve engine efficiency through structural modifications and engineering innovations [10-11].

In this context, the application of ceramic coatings in IC engines is considered a promising solution. Ceramic coatings act as efficient insulators, reducing the amount of heat transferred from the engine's cooling system to the cylinder. Researchers are predominantly focused on eliminating the necessity for a cooling system in internal combustion engines. By doing so, it is expected that both the cost and weight of the engine will minimized , while simultaneously enabling higher levels of efficiency [12].

Several ceramic coatings have been utilized in the advancement of engine technology. Partially stabilized zirconia (PSZ), typically containing 6-9% stabilizing elements, has been a prominent choice. Yttria-stabilized zirconia (YSZ) is the most widely used material for thermal barrier coatings (TBCs) and has demonstrated superior performance at elevated temperatures. Nevertheless, alternative TBC options like mullite, calcium/magnesium-stabilized zirconia (Ca/Mg-PSZ), aluminum oxide (Al_2O_3), and titanium dioxide (TiO_2) show promise due to their specific attributes suited for engine development [13].

Literature findings indicate that the primary limitation of using 7% YSZ (yttria-stabilized zirconia) occurs when exposed to temperatures exceeding 1200°C, resulting in undesirable phase transitions that lead to the formation of cracks on the top surface. Current advancements in the quest for an alternative to YSZ as a ceramic topcoat have unveiled a range of innovative ceramics, including rare earth oxides, which exhibit better performance at temperatures surpassing 1200°C [14].

As an illustration, rare earth oxides such as Gd_2O_3, Yb_2O_3, and Nd_2O_3 have been found to exhibit lower thermal conductivity compared to YSZ. This reduction in thermal conductivity is achieved by introducing two or more oxides into zirconia. The combination of these dopants can reduce thermal conductivity by approximately 15-30% when compared to YSZ ceramics. Additionally, they enhance the sintering stability of the coating at elevated temperatures.

The current study examined how alumina nanoparticle affected the B20 (10% Calophyllum inophyllum and 10% Macadamia) biodiesel's combustion, performance, and emission. As test samples, alumina nanoparticles 25ppm was used, specifically B20 + 25 ppm,. The ASTM method was used to assess the properties and characteristics of the test fuel.. Further current research was carried out to enhance engine performance by providing different thermal barrier coating(TBC) on standard pistons. For varying load conditions, the engine oprated at an invariant speed of 1500 rpm.

2. Materials Method

2.1 Preparation of LHR system

In this investigative analysis, the plasma spray system is employed for applying the coating depicted in Fig. 1. The details regarding the plasma spray system are presented in Table 1. Currently, the Ni-Cr-Al-Y system is applied as a bond coat with a thickness of 50µm on two distinct pistons. For the top coat layer comprises of a 250 microns (0.25 mm). The top ceramic coat materials are 2% Nd + YSZ (CP1) and 2% Gd + YSZ (CP2) were employed because of their elevated melting point and reduced thermal conductivity. Figure 2 displays images of pistons with various TBC coatings, including snapshots of the STD-coated pistons.

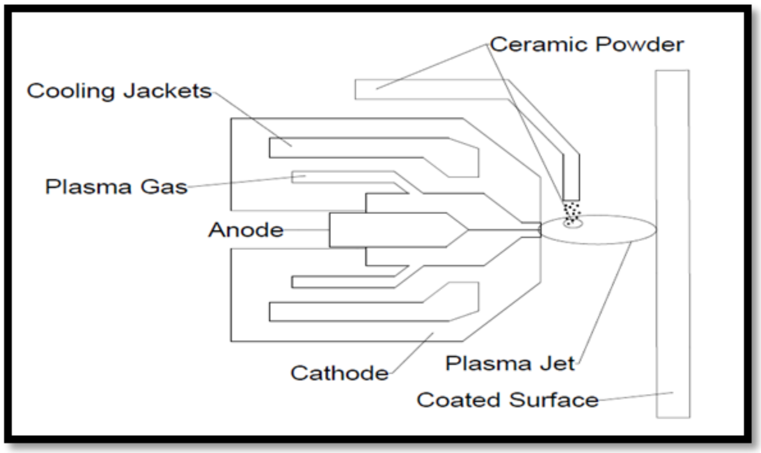

Fig.1. Plasma spray coating system

Table.1 Particulars of plasma spray system

Coating parameters	**Specifications**
Pressure : hydrogen gas	60 PSI
Spraying distance	2.5–4 in
Plasma gun	3MB plasma spray gun
feed rate of powder	35–45 g per minute
Pressure of argon gas	95–120 PSI
Nozzle	GH Type nozzle
Flow rate of argon gas	85–905 LPM
Flow rate of hydrogen gas	14–17 LPM

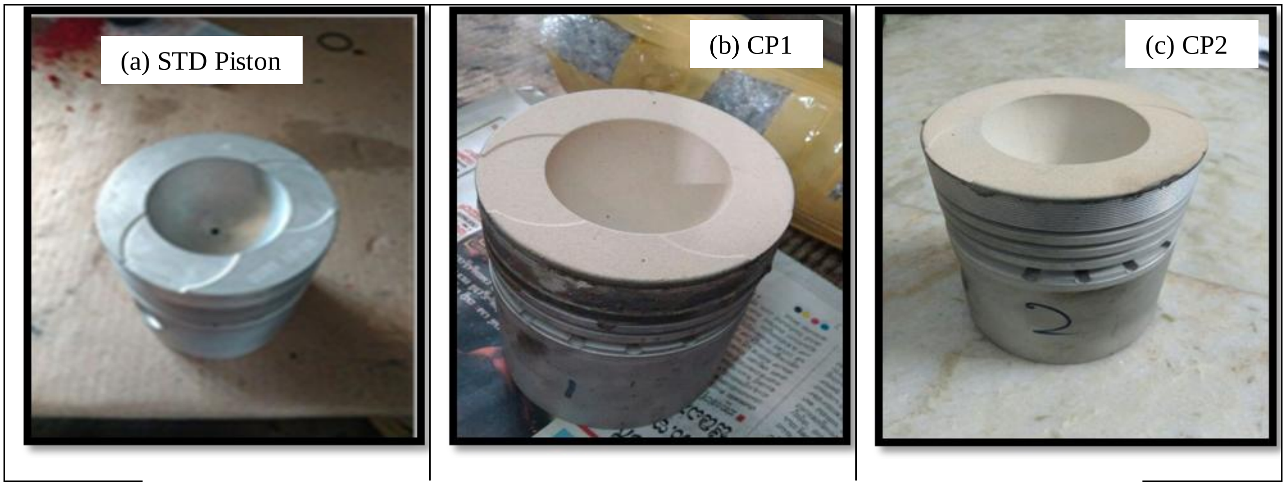

Fig.2. (a) photographic view of uncoated STD engine piston and (b, & c) Coated pistons

2.2 Selection of Biodiesel

As the primary source of energy for industrial needs, researchers are working hard to find a sustainable alternative to the current fossil fuels. The study of alternative fuel combustion is currently receiving a lot of attention in an attempt to become the most promising diesel fuel replacement in the transportation sector. Because of the wide variations in their composition and the lack of data from experiments on the responses that comprise the literature, it is still hard to predict the eventual combustion characteristics of this fuel [15-22].

2.3 Callophyllum Inophyllum oil

Calophyllum inophyllum, sometimes known as polanga, is a non-edible oilseed decorative evergreen tree that belongs to the clusiaceae family. Kamani, Alexandrian laurel, honne, tamanu,pinnai, and other names have been given to it in different parts of the world. They usually grow best in deep soil or on open sea beaches, and they need from 750 to 5000 mm of rain every year to thrive. India, Eastern Africa, Southeast Asia, and Australia are among places where this plant has been found. The tree produces 100 to 200 fruits every year, with an oil yield of 2000 kg per hectare. Oil with a high percentage of 65 to 75% is produced from the seed, which is coloured green and thick, with a woodsy or nutty aroma.

2.4 Macadamia Integrifolia oil

The macadamia nut tree, scientifically known as Macadamia integrifolia, is a large, spreading evergreen tree that can grow to a height of 30-50 feet. Its natural habitat is the rainforests of southeastern Queensland, Australia [28]. The macadamia nut has a long history of being used as a food source by Aboriginal people in Australia, well before the arrival of Europeans. In 1837, this tree was introduced to Hawaii for the first time. The macadamia nut tree (Macadamia integrifolia) features glossy leaves that are oblong-lanceolate to oblong-ovate in shape, measuring around 8-10 inches in length. The margins of the leaves are slightly wavy. The leaves

grow in whorls of three, creating an attractive foliage arrangement. Hand nutcrackers can crack the shells because they are too hard. Powerful husking machines are used to open commercial fruits.

2.5 Calophyllum Inophyllum and Macadamia transesterification process

A 100 mL of Calophyllum oil was determined and taken into a 250 ml conical flask and heated to a temperature of 50° C. The amount of Ethanol was taken into a round bottom flask and the heater was on. It was complete to purify Ethanol. (30ml).The sodium hydroxide NaOH pellet was placed in the weighting stability to get exactly 0.25g. The mixture of ethanol and NaOH catalyst is added by using a pipette into a solution of Calophyllum oil. After adding the solution, it should be magnetic stirred at room temperature and the maximum time is half-hour. After that the tested fuel was taken into ultrasonicator for better mixing for maximum of 45minutes. The combination was then given a 24-hour period in a separating funnel to settle.The bottom layer, which is prepared up of glycerol and soap, was then gathered from the bottom of the separating funnel, and the biodiesel was then put into a separate beaker.

After that, the biodiesel was washed off in warm water in order to take out any remaining glycerol and soap in the funnel. As soon as pure water could be seen beneath the biodiesel in the separating funnel, it was finished. The surplus water still exist in the biodiesel was eliminated, and the cleaned sample was dried by setting it on a hot plate. The amount of biodiesel that was gathered was measured and noted. The same procedure is repeated for Macadamia oil.

Table.2 Fuel Properties

Properties	**Diesel**	**B_{20}+80D**	**B_{20}+80D 25+ppm**

Calorific value (MJ/Kg)	44.5	41.605	43.67
Cetane number	55	53	52
Density (kg/m^3) @ 15 °C	831	859	851.7
Kinematic viscosity (cSt) @ 40 °C	2.14	3.28	3.31
Flash point (^{O}C)	52	76	82

2.6 Synthesis and Characterization of Al_2O_3nano particle:

Synthesis of nanoparticles and preparation of blends Using the sol-gel combustion method, which involves blending a 0.5 M aluminium nitrate solution in 50 ml of H_2O at 22 °C and stirring it with a magnetic stirrer, Al_2O_3 nanoparticles were created. After that, aluminium nitrate and 0.05 M urea are combined, and the mixture is treated for 30 minutes to reach a pH 2 solution. The pH 6 solution was reached by further titrating with 25 ml of H2O and 0.1 M sodium hydroxide. Al_2O_3 nanoparticles were obtained in a container and allowed to air out at 300 °C for two hours in the furnace after the sample was dried at 150 °C for 12 hours following the development of clady gel (pH = 8) with sodium hydroxide addition. Table 3 provided specifics about the physical characteristics of the produced Al_2O_3 nanoparticles. Figure 3 showing XRD for the particle size assessment and Figure.4 and Figure.5 shows the SEM , EDAX spectroscopy of synthesized Al_2O_3 nanoparticles. A spherical structure with few groups is visible in these images. The sample's particle size falls between 10 and 20 nm, which is in good accordance with the findings analyzed from XRD investigations. The synthesized Al_2O_3 nanoparticles were blended with The 10% of Calophyllum biodiesel & 10% of Macadamia Biodiesel blend (B20) was developed on a volume basis. The nano fuel was formulated by dispersing Al_2O_3 nanoparticles, prepared previously, into the B20 blend at mass fractions of 25 ppm using an ultrasonicator device. Subsequently, the resulting nano fuel was mixed with 80% diesel employing a mechanical stirrer. The fuels used in the current study were prepared as follows: a blend consisting of 10% Calophyllum biodiesel and 10% Macadamia biodiesel, combined with 80% diesel (referred to as B20+80D), and a mixture including 25 ppm of Al_2O_3 nanoparticles with the 10% Calophyllum biodiesel and 10% Macadamia biodiesel blend, also with 80% diesel (referred to as B20+25ppm). To enhance the stability of dispersed nanoparticles, a surfactant of 0.1 mg per liter is introduced. The surfactant used in this study is CTAB (cetyltrimethylammonium bromide). The biodiesel blend with nanoparticles remained stable for over 96 hours. Engine testing was conducted only after confirming the stability of the nanoparticles [23,25,30,31].The complete fuel properties (tested) are represented in Table.2.

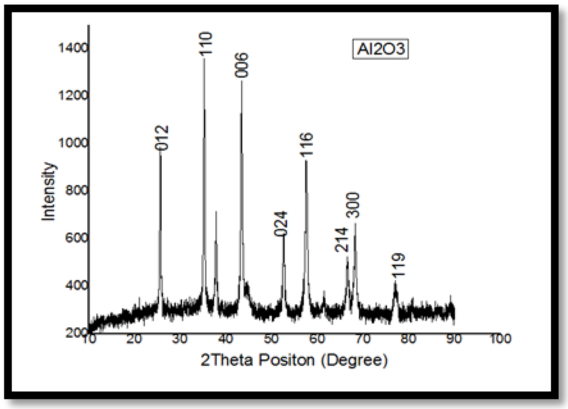

Fig. 3. XRD analysis of Al_2O_3 Nanoparticles.

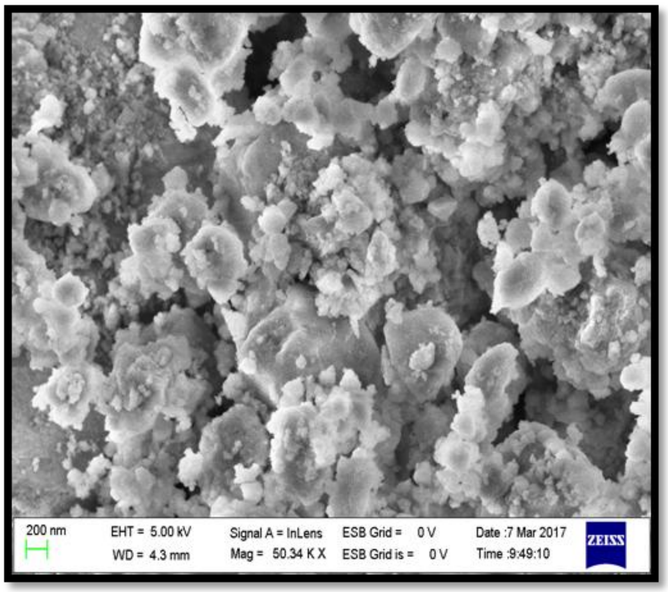

Fig.4. SEM image of Al_2O_3 Nanoparticles.

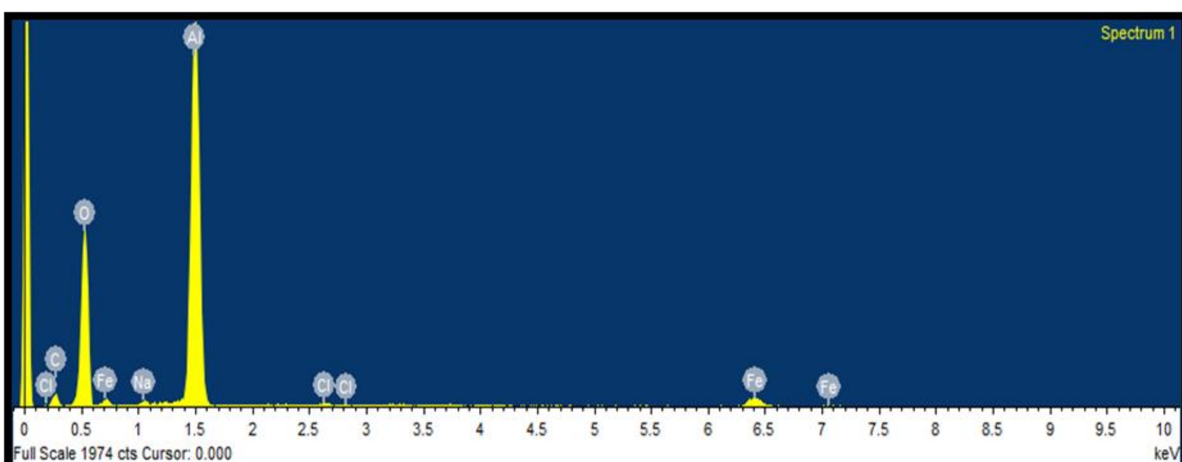

Fig. 5. EDAX report on Al_2O_3 Nanoparticles.

Table 3 Particulars of alumina Nanoparticles

Type	Size	Purity	SSA	Color
Aluminium oxide nanoparticle (Al_2O_3, gamma)	20 nm	+99%	>138m^2/g	White

3. Experimental Test Setup

The study employed a DI diesel engine that is mono-cylinder, vertical, and air-cooled. This engine, operating at 1500 rpm, has a peak power output of 5.1 kW and was connected to an eddy current dynamometer. The engine's inlet configuration includes an anti-pulsation chamber, an air heater, and a device to assess the air temperature. To measure exhaust gas temperature (EGT), chromel-aluminum (k-type) thermocouples were affixed to the exit pipe. Fuel flow was quantified using a stopwatch and a 10 cc graded burette. For the measurement of cylinder pressure, a piezoelectric pressure transducer can be affixed to the cylinder's top surface.

Calculations were performed to analyze combustion parameters, including ignition delay, inside pressures (CP), highest rate of pressure increase, heat release (HRR), and cumulative heat release (CHRR). For detailed information about the test engine, refer to Table 4. A conceptual image of the engine configuration is presented in Figure 6.

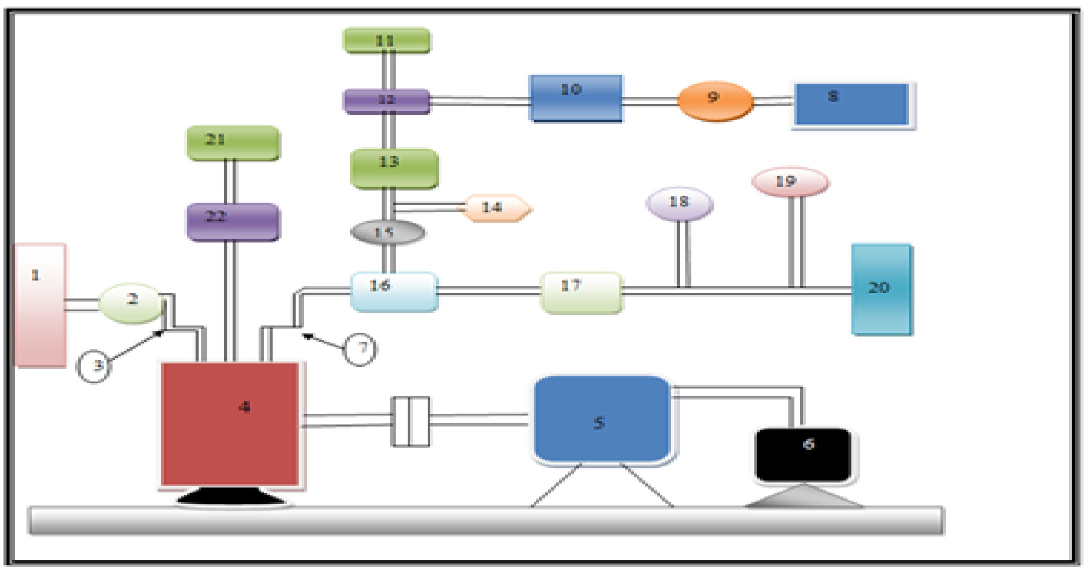

Fig.6 schematic diagram of engine set up

1. &2. Air tank and Filter 3. Inlet manifold 4. Test Engine 5. Dynamometer 6. Loading apparatus 7. Exhaust Manifold 8. Urea Tank 9. Engine Motor 10. Pressure Relief Valve 11. Battery 12. Relay 13. Heater 14. Pressure Gauge 15. Solenoid Valve 16. Mixing Chamber 17. SCR Catalyst 18. Five Gas Analyser 19. Smoke-meter 20. Exhaust Gas

Table 4. Technical details of the Engine

Engine Make	**Kirloskar TAF1**
Type	Vertical diesel engine, four stroke
No. of Cylinders, Fuel	One, Diesel
Cooling System	Air cooled
Ignition system	Compression ignition
Rated brake power	4.4 kW @ 1500 rpm
Displacement	661 cc
Bore and stroke	87.5 mm and 110 mm
Compression ratio	17.5:1
Injection timing	23° bTDC (rated)
Injection pressure	200 bar

4.Results and Discussions:

4.1 Performance parameters

The primary focus of this study revolves around both the standard Engine and TBC coated Engines, denoted as CP-1 and CP-2. These engines were operated using diesel, B20, and B20+25ppm Al2O3 nano additive as the fuel. In the present study, the experiments were paying attention on performance variables (BTE, and BSFC), Combustion parameters (CP, HRR, and EGT), pollutant characteristics (HC, CO, Smoke, and NOx) Outcome of these studies will fetch out the assessment of the performance amongst the STD engine and TBC coated engines using different fuel samples.

4.1.1. Brake Thermal Efficiency (Bte).

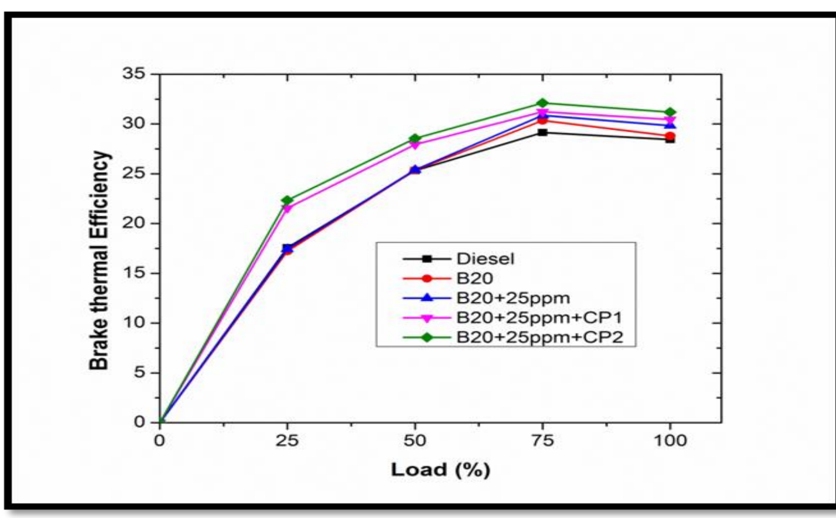

Fig.7 distinguish between BTE Vs Load

Figure 7 illustrates the difference in BTE as it relates to the load in both the Standard and coated engines, utilizing Diesel, B20, and B20+25ppm as fuels. The testing outcome exhibits that at maximum load condition the BTE for STD diesel fuel,B**2**0, B20+25ppm Al_2O_3 nanoadditive in CP1 and CP2 engines are found to be 28.44%, 28.8%, 28.98%, 30.45% and 31.2%. while compared with the standard diesel fuel, there was an increase in BTE of 1.54%, 1.89%, 7.06%, and 9.7%, respectively. The maximum BTE was found in CP2 engine while equated with other engines. This result was ascribed to the inclusion of alumina nanoparticles, which function as fuel boosters and oxygen buffers, causing full combustion and raising thermal efficiency[24,26]. This effect might arise from the TBC material's low thermal conductivity, which elevates the thermal resistance over the piston's surface. This increased resistance further contributes to improved thermal efficiency due to retained heat. The reason behind this is due to co-doping the low thermal conductivity rare earth oxides in to YSZ, which leads the higher concentration of oxygen vacancies in the coating combination and would lead to a stronger dispersion of the phonon, which could curtail thermal conductivity of the TBC materials when compared to other engines [27-29]

4.1.2 Brake Specific Fuel Consumption

Figure 8 demonstrates the distinction in BSFC concerning load in both the STD and ceramic engines, utilizing Diesel, B20, and B20+25ppm as fuels.. It is noted that STD diesel fuel,B20, B20+25ppm Al_2O_3 nanoadditive in CP1 and CP2 Engines shows minimum BSFC values of 0.299 kg/kWhr,0.28 kg/kW.hr,0.266 kg/kW.hr,2.5 kg/kW.hr,2.3 kg/kW.hr respectively. In comparison to standard diesel, a reduction in BSFC was observed at rates of 6.78%, 11.03%, 16.38%, and 23.07%, respectively. BSFC is inversely related to BTE, and as a result, all LHR Engines exhibit superior reductions in BSFC when equated with the standard engine[32]. The reduction in BSFC is due to a decline in fuel consumption and an increased level of energy conversion in the coated engine under every load setting. This effect may be attributed to the inclusion of low thermal conductivity dopants in the LHR engine. These dopants enhance heat resistance, raising the temperature in the combustion chamber, and subsequently increasing the fuel temperature within the cylinder [27-29].

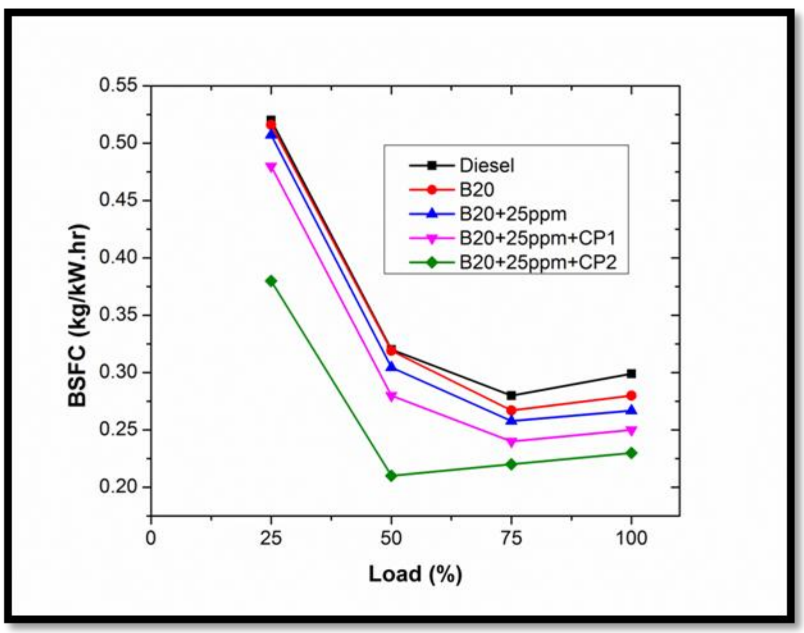

Fig.8. distinguish between BSFC Vs Load

4.2 Combustion Analysis

4.2.1 Exhaust Gas Temperature

Figure 9 demonstrates the distinction in outlet gas temperature at different loads for the standard piston using diesel fuel, as well as B20 and B20+25ppm in both LHR Engines. Coated Engines shows the higher E.G.T than the STD engine operating with diesel fuel. At peak load condition, EGT shows that the diesel fuel with STD engine is 407^{o}C. whereas B20 and B20+25ppm nano additive ,LHR 1 and LHR2 Engines was found to be 411^{o}C, 424^{o}C, 445^{o}C, and 472^{o}C respectively. This proves that LHR Engines exhibit higher EGT than the standard engine. EGT is directly associated with the combustion temperature. Consequently, one can anticipate an increase in EGT in TBC engines. Moreover, elevated combustion temperatures might also impact the content and volume of the gases expelled through the outlet [26,27].

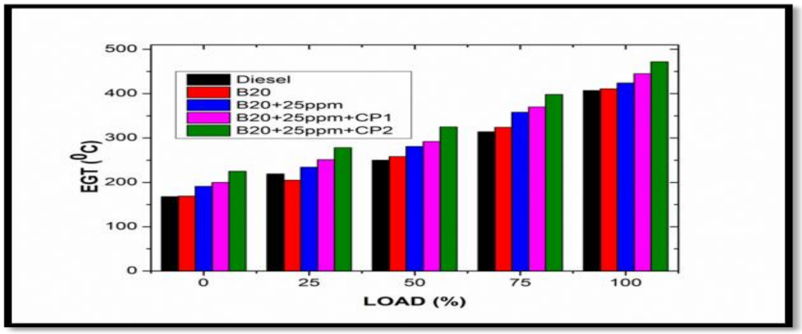

Fig.9 distinguish between EGT Vs Load

4.2.2 Cylinder Pressure

Figure 10 showcases the fluctuation in cylinder pressure concerning the crank angle in both the standard and coated engines, employing diesel fuel, B20, and B20+25ppm in the LHR Engines. The CP1 and CP2 Engines achieved higher peak cylinder pressure in comparison to the standard engine. An observed rise in cylinder pressure of 4.5%, 6.2%, 8.1%, and 12.6%, respectively, was noted when equated with standard engine. The engines with coatings resulted in heightened peak pressure inside the cylinder. During the initial mixing phase, more fuel may possibly consumed, thereby generating increased heat in TBC engines [27,28].

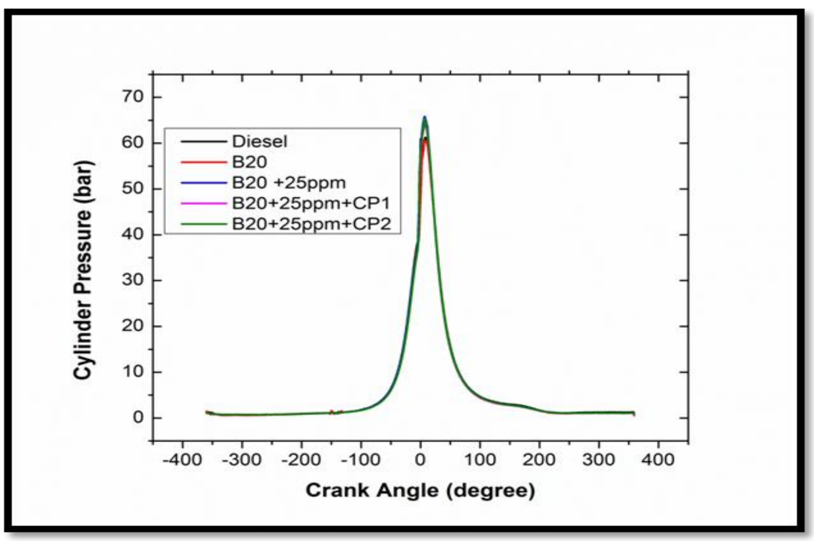

Fig.10. distinguish between Cylinder Pressure Vs Load

4.2.3 Heat Release Rate

Figure 11 illustrates the distinction in Heat Release Rate in relation to the crank angle for both the STD and coated engines under maximum loading conditions, using diesel fuel, B20, and B20+25ppm. The rise in HRR for coated Engines was determined to be 4.9%, 6.8%, 7.4%, and 13.1%, respectively, equated with standard engine. It can be said that the prole had an increased rate of heat release since of the greater fuel formation and the shorter ignition delay with alumina nanoparticle [30-32]. The another reason for the heightened HRR is attributed to the thermal protection provided in the piston crown, which tends to result in higher HRR in ceramic engines. HRR serves the purpose of detecting the initiation of combustion, determining the portion of fuel burnt during the premixed combustion phase, and distinguishing variations in fuel combustion rates. A shorter delay in ignition might be happens because of higher cetane number and vice versa. The cetane number is a major pointer of the fuel used in engine and it is a dimensionless descriptor [27,29,30].

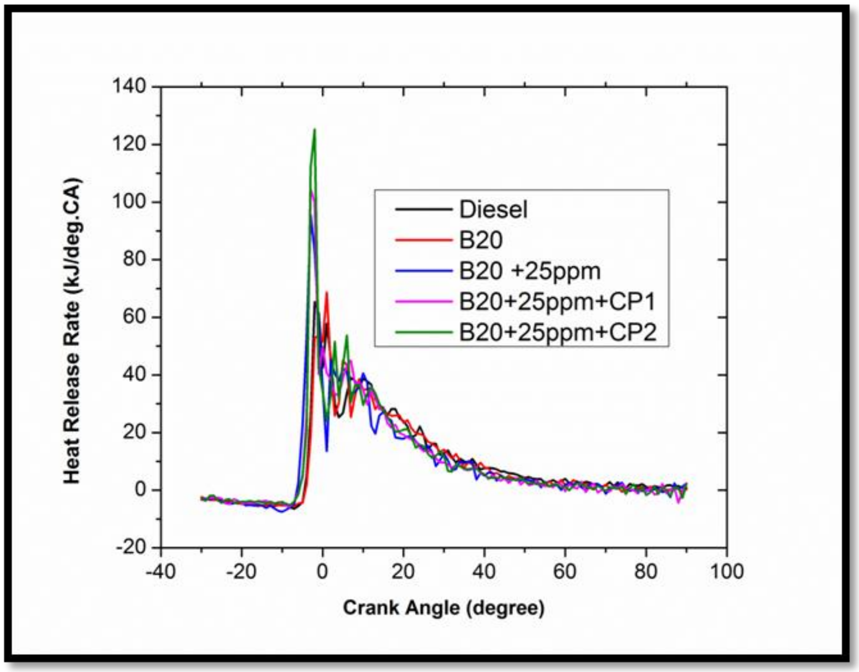

Fig. 11 distinguish between HRR Vs Load

4.3 Emission characteristics

4.3.1 Hydrocarbon

Figure 12 illustrates the distinction in HC emissions at various loads in both the standard and coated engines using diesel , B20, and B20+25ppm. The test results show that at maximum load conditions, HC emissions for STD diesel, B20, B20+25ppm nanoadditive, CP1, and CP2 Engines were measured at 22 ppm, 19 ppm, 16 ppm, 15 ppm, and 13 ppm, respectively. It is confirmed that engines with coatings exhibit lower HC emissions compared to the standard engine. The decrease in HC was found to be 13.6 %, 27.27 %, 31.81% and 38.25% equated with normal Engine. This might be the result of the alumina nanoparticle's high active energy and plentiful oxygen molecules, which decreased the amount of carbon deposited in the cylinder wall[30] .This occurs due to the heightened combustion temperatures in TBC engines, leading to the incineration of hydrocarbons in the fuel and subsequently reducing unburned hydrocarbon emissions. Emission of HC gases is triggered by incomplete fuel combustion. In a coated engine, the likelihood of HC emissions is reduced, thanks to a smaller quenching distance and a lower flammability limit combined with the combustion of LHR engines. [27,33,28].

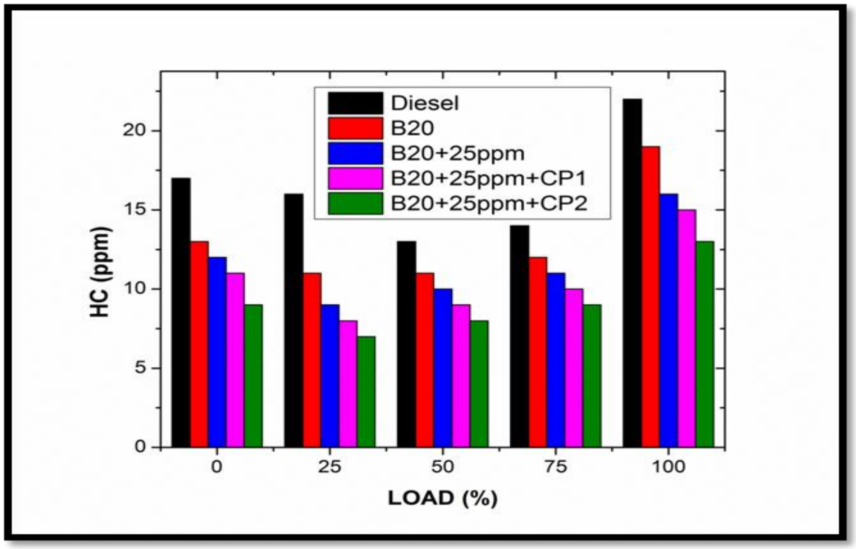

Fig.12 distinguish between HC Vs Load

4.3.2 Carbon Monoxide

Figure 13 exhibits the fluctuations in CO pollutant at various loads in both the standard and ceramic engines, employing diesel fuel, B20, and B20+25ppm nanoadditive. The experimental findings confirm a reduction in CO emissions for B20+25ppm in CP1 and CP2 Engines compared to the STD engine. There was an observed reduction in CO emissions by 11.6%, 14.36%, 21.2%, and 24.6%, respectively, in comparison to the STD engine. In engines with coatings, the inclusion of TBC coating contributes to enhanced combustion, leading to a decrease in CO emissions. This reduction is a result of incomplete combustion and various factors, predominantly air-fuel density and cylinder temperatures [26,33,34].

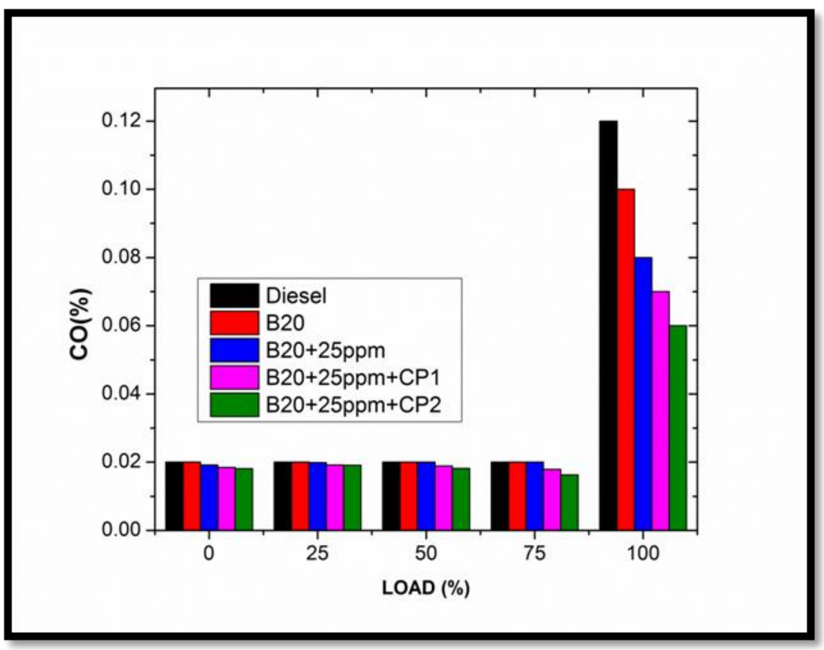

Fig.13 distinguish between CO Vs Load

4.3.3 OXIDES OF NITROGEN

Figure 14 displays the variations in NOx pollutant at various loads in the standard and ceramic engines, employing diesel , B20, and B20+25ppm nanoadditive. Under initial load conditions, it has been identified that NOx emissions were low and enhanced as the load was raised. The heightened intake of fuel and a richer combustion process were the contributing factors for the enhanced NOx emissions at maximum loads. The research results confirm that at peak load conditions, NOx emissions using B20+25ppm nano additive for CP1 and CP2 Engines increase compared to the STD engine. There was an observed rise in NOx of 4.8%, 21.2%, 28.3%, and 30.45%, respectively. Typically, the B20 + 25 ppm blend produces higher NOx emissions because of better combustion brought on by the alumina nanoparticles' ability to donate oxygen (rlk). The NOx pollutant in coated engines are notably higher when equated with standard engine. [15,27,33,34].

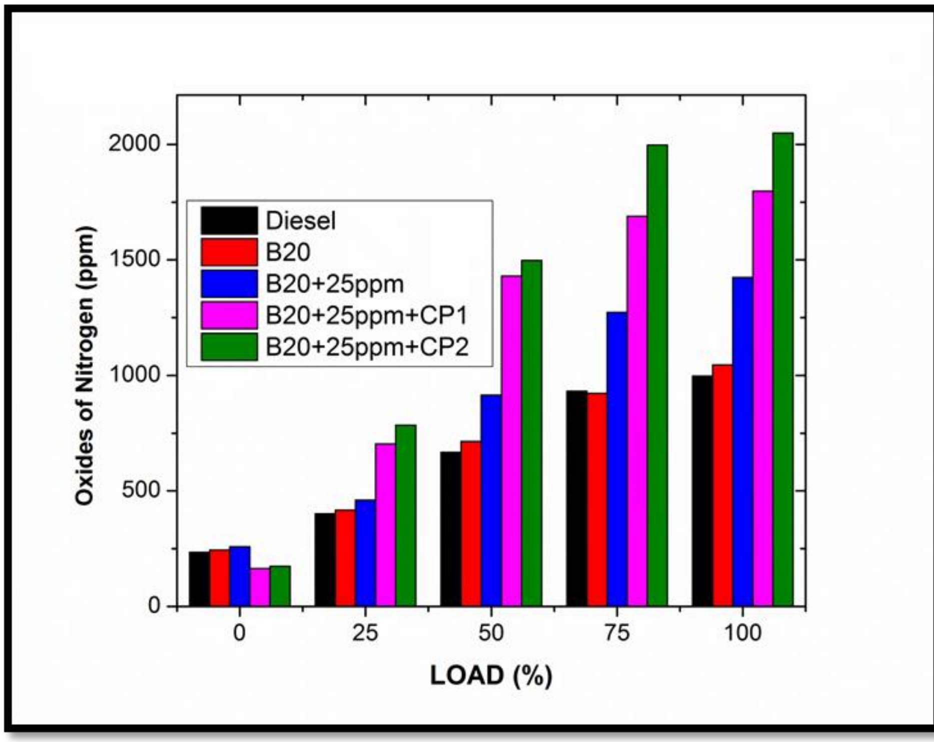

Fig.14 distinguish between NOx Vs Load

4.3.4 SMOKE OPACITY

Figure 15 depicts the distinctions in smoke opacity with regard to different loads in both the standard and LHR engines fuelled with diesel, B20, and B20+25ppm nanoadditive. The investigational results validate that under peak load conditions, the smoke opacity for B20+25ppm nanoadditive in CP1 and CP2 decreases compared to the STD Engine. There was an observed reduction in smoke opacity of 6.28%, 7.6%, 9.4%, and 11.3%, respectively, in comparison to the STD Engine. In the meantime, full combustion and the removal of carbon deposition were produced by the oxygen involvement in the biodiesel and the impact of alumina nanoparticles [33,34]. These are the potential causes of the B20 + 25 ppm blend's reduced smoke emissions. This occurs due to effective ignition and improved air-fuel mixture in LHR Engines, which are liable for the reduction in smoke emissions [28-29].

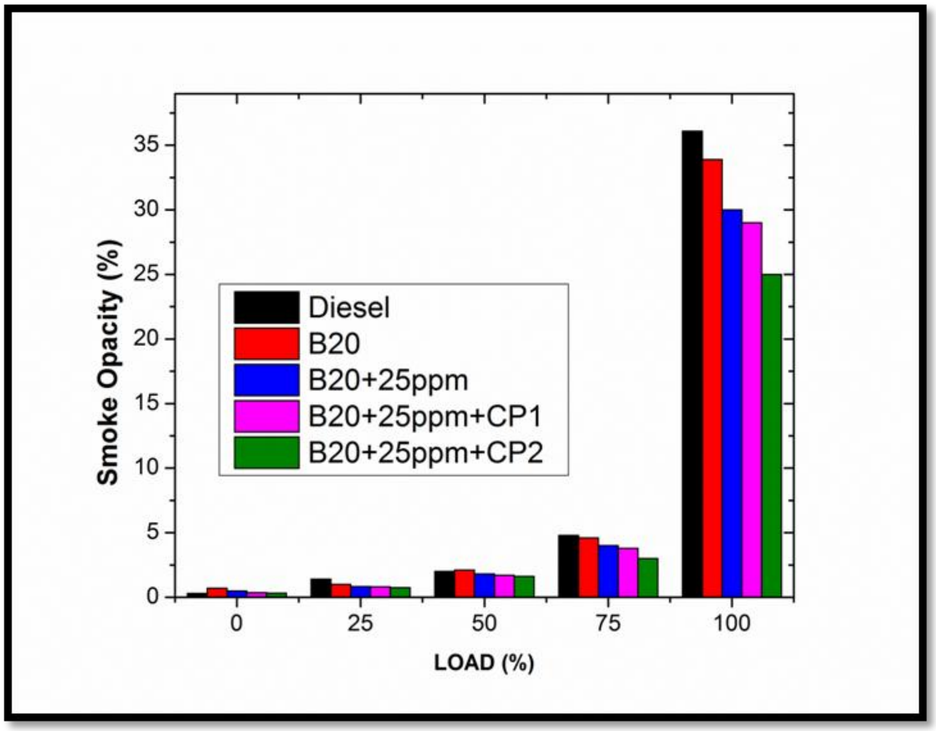

Fig.15 distinguish between Smoke Opacity Vs Load

5. Conclusion

The study examines a standard diesel engine using diesel fuel, B20, and B20+25ppm nanoadditive, where ceramic coatings (CP1 and CP2) are applied to the piston crown via a plasma spray method with a 250-micron layer. Engine parameters such as BTE, BSFC, EGT, as well as emissions such as HC, CO, Smoke, and NOx, are evaluated in this exploration.

- BTE showed increases of 1.54%, 1.89%, 7.06%, and 9.7%, respectively, when equated with standard engine. Among the tested conditions, the CP2 engine with the nanoadditive exhibited the highest BTE..
- There was a reduction in BSFC by 6.78%, 11.03%, 16.38%, and 23.07%, respectively, in comparison to STD diesel. Among the tested conditions, the CP2 engine showed the highest BSFC reduction.
- It is confirmed that ceramic coated engines exhibit higher EGT than the other engines..
- The uppermost peak cylinder pressure was achieved by CP1 and LCP2 engines in equated to the standard engine. The observed increase in cylinder pressure amounted to 4.5%, 6.2%, 8.1%, and 12.6%, respectively, when compared to the standard engine using diesel fuel.
- The highest HRR was achieved with B20, B20+25ppm nanoadditive in CP1 and CP2 Engines, surpassing the standard engine. It is observed that the enhancement in HRR for the coated Engines amounted to 4.9%, 6.8%, 7.4%, and 13.1%, respectively, equated to the standard engine using diesel fuel.
- It is confirmed that ceramic engines exhibit lesser HC emissions equated with standard engine engine. The observed reductions in HC were 13.6%, 27.27%, 31.81%, and 38.25% in comparison to the STD Engine.
- The investigational results validate a curtailed in CO emissions for B20+25ppm in CP1 and CP2 Engines compared to the STD engine. The recorded CO reductions were 11.6%, 14.36%, 21.2%, and 24.6% respectively.

- This study proves that at full load conditions, NOx emissions increased for B20+25ppm nano additive in CP1 and CP2 Engines compared to the STD engine. The recorded increases in NOx were 4.8%, 21.2%, 28.3%, and 30.45%, respectively.
- The investigational results validate that under peak load conditions, the smoke opacity for B20+25ppm nanoadditive in CP1 and CP2 engines decreases compared to the standard engine. The observed reductions in smoke opacity were 6.28%, 7.6%, 9.4%, and 11.3%, respectively, while compared to the standard engine.

Nomenclature:	
TBC Thermal Barrier Coating	EGT Exhaust Gas Temperature
YSZ Yttria-Stabilized zirconia	Gd_2O_3 Gadolinium Oxide
Nd_2O_3 Neodymium oxide	STDE Standard Engine
IC Internal Combustion	CI Compression Ignition
BTE Brake Thermal Efficiency	DI Direct Injection
CP Coated piston	CI Compression Ignition
LHR Low Heat Rejection Engine	Al_2O_3 Aluminium oxide

References

[1] Aggarwal, S. K., F. Xiao, and S. Wijeyakulasuriya. 2016. Effects of fuel reactivity and injection timing on diesel engine combustion and emissions. International Journal of Green Energy 13 (5):431–45. doi:10.1080/15435075.2014.961469.

[2] Datta A, Mandal BK (2017) An experimental investigation on the performance, combustion and emission characteristics of a variable compression ratio diesel engine using diesel and palm stearin methyl ester. Clean Techn Environ Policy 19:1297–1312. https://doi. rg/10.1007/s10098-016-1328-3

[3] Chuah LF, Aziz ARA, Yusup S et al (2015) Performance and emission of diesel engine fuelled by waste cooking oil methyl ester derived from palm olein using hydrodynamic cavitation. Clean Techn Environ Policy 17:2229–2241. https://doi.org/10.1007/s10098-015-0957-2

[4] Capuano D, Costa M, Di Fraia S et al (2017) Direct use of waste vegetable oil in internal combustion engines. Renew Sust Energ Rev 69:759–770. https://doi.org/10.1016/j.rser.2016.11.016.

[5] Lingesan, S., K. Annamalai, M. Parthasarathy, K. M. Ramalingam, B. Dhinesh, and J. Isaac Joshuaramesh; Lalvani. 2018. Production of Garcinia gummi-gutta methyl ester (GGME) as a potential alternative feedstock for existing unmodified DI diesel engine: Combustion, performance, and emission characteristics. Journal of Testing and Evaluation 46 (6):20170246. doi:10.1520/JTE20170246.

[6] Maawa, W. N., R. Mamat, G. Najafi, and L. P. H. De Goey. 2020. Performance, combustion, and emission characteristics of a CI engine fueled with emulsified diesel-biodiesel blends at different water contents. Fuel 267 (November 2019):117265. doi:10.1016/j. fuel.2020.117265.

[7] Janakiraman S, Lakshmanan T, Chandran V, Subramani L (2020) Comparative behavior of various nano additives in a DIESEL engine powered by novel Garcinia gummi-gutta biodiesel. J Clean Prod 245:118940. https://doi.org/10.1016/j.jclepro.2019.118940.

[8] Dash SK (2020) Effect of CR on the performance, emission and heat release rate of a DI diesel engine run by B20 blend of waste cooking biodiesel in diesel fuel. In: Ghosh S., Sen.

[9] H. Tarigonda, V.Gangula, R. krupakaran, H. Tarigonda, L. Kala, R. Doddipalli, Effect of TBC, Turbocharger and EGR on the Performance of Diesel Engine Using Biodiesel, SAE Technical Paper 2022-28-0558, 2022, Doi: 10.4271/2022- 28-0558.

[10] V. Gangula, R. Krupakaran, H. Tarigonda, L. Kala, R. Doddipalli, Optimization of the Effect of Low Heat Rejection Diesel Engine Using Biodiesel with Taguchi Method, SAE Technical Paper 2022-28-0577, 2022, Doi: 10.4271/2022-28- 0577.

[11] G. Vidyasagar Reddy, N. GovindhaRasu, T. Hari Prasad, Experimental Analysis and Energy Balance on Thermal Barrier-Coated Piston Diesel Engine Using Biodiesel, J. Institut. Engineers (India): Ser. C (2020) 1–12.

[12] G. Vidyasagar Reddy, N GovindhaRasu, T. Hari Prasad, Investigation on Different Thermal Barrier-Coated Piston Engines Using Mahua Biodiesel, J. Instit. Engineers (India): Ser. C (2020) Doi: 10.1007/s40032-020-00621.

[13] G. Vidyasagar Reddy, R.L. Krupakaran, Hariprasad Tarigonda, D. Raghurami Reddy, N. GovindhaRasu, Energy balance and emission analysis on diesel engine using different thermal barrier coated pistons, Mater. Today: Proc. 43 (Part 1) (2021) 646–654, ISSN 2214-7853.

[14] S. Maghsoodloo, G. Ozdemir, V. Jordan, C.-H. Huang, Strengths and limitations of taguchi's contributions to quality, manufacturing, and process engineering, J. Manuf. Syst. 23 (2) (2004) 73–126.

[15] R. Krupakaran, V. Gangula, H. Tarigonda, L. Kala, R. Doddipalli, Optimization of Operational Parameters on Engine Performance and Emissions of a Diesel Engine Powered with Mimusops Elengi Methyl Ester with Doped TiO2 Nanoparticle with Varying Injection Pressure, SAE Technical Paper 2022-28-0574, 2022, Doi: 10.4271/2022-28-0574.

[16] Li, S.; Wang, Y.; Dong, S.; Chen, Y.; Cao, F.; Chai, F.; Wang, X.: Biodiesel production from Eruca Sativa Gars vegetable oil and motor, emissions properties. Renew. Energy 34(7), 1871– 1876 (2009)

[17] Qi, D.H.; Lee, C.F.; Jia, C.C.; Wang, P.P.; Wub, S.T.: Experimental investigations of combustion and emission characteristics of rapeseed oil–diesel blends in a two cylinder agricultural diesel engine. Energy Convers. Manag. 77, 227–232 (2014)

[18] Dhar, A.; Kevin, R.; Agarwal, A.K.: Production of biodiesel from high-FFA neem oil and its performance, emission and combustion characterization in a single cylinder DICI engine. Fuel Process. Technol. 97, 118–129 (2012).

[19] Dubey, Pankaj. and Gupta, Rajesh. (2017), 'Influences of dual bio-fuel (Jatropha biodiesel and Turpentine oil) on single cylinder variable compression ratio diesel Engine', *Renewable Energy* **115**, 1294-1302

[20] Duraisamy, M.K., Balusamy, T. and Senthil kumar, T. (2011), 'Reduction of NOx emissions in Jatropha seed oil fuelled CI Engine', *ARPN Journal of* Engine*ering and Applied Science* **6**(5), 34-9.

[21] Maharaja, Gasti. and Navindgi, M.C.(2013), 'Comparative experimental investigation of performance and combustion characteristics in a single cylinder thermal barrier coated diesel Engine using diesel and Castor biodiesel', *International Journal of* Engine*ering Research and Technology* **2**(7), 503-511.

[22] Nalgundwar, A., Paul, B. and Sharma, S.K. (2016), 'Comparison of performance and emissions characteristics of DI CI Engine fueled with dual biodiesel blends of palm and jatropha', *Fuel* **173**, 172-179.

[23] Nayak, S. and Pattanaik, B. (2014). 'Experimental Investigation on Performance and Emission Characteristics of a Diesel Engine Fuelled with Mahua Biodiesel Using Additive'. *Energy Procedia* **54**(0), 569-579.

[24] Piramanandhan, M., Raju, N.M.S. and Venkatesan, R. (2016), 'Performance and Emission Characteristics of Multilayer Thermal Barrier Coated Di Diesel Engine Fuelled With Sunflower Bio Diesel', *International Journal of Applied Environmental Sciences* **11**(1), 267-278.

[25] Prabhahar, M. and Rajan, K. (2013), ‘Performance and combustion characteristics of a diesel Engine with titanium oxide coated piston using Pongamia methyl ester’, *Journal of mechanical science and technology* **27**(5), 1519-1526.

[26] Rao, N., Krishna, M., Chowdary, R., Janardhan, N., Rao, V. and Reddy, T. (2018),‘Experimental investigations on pollution levels from supercharged partially adiabatic diesel Engine with tamarind biodiesel blended with diethyl ether’, *Pollution Research* **37**, 235-240.

[27] Vikrant Garud., Sanjiwan Bhoite., Suraj Ghadage., Nilesh Gaikwad., Devesh, Kute. and Sivakumar, G. (2017), ‘Performance and Combustion Characteristics of Thermal Barrier Coated (YSZ) Low Heat Rejection Diesel Engine’, *Materials Today proceedings* **4** (2), 188-194.

[28] Buyukkaya, E.: Effects of biodiesel on a DI diesel engine performance, emission and combustion characteristics. Fuel 89, 3099– 3105 (2010)..

[29] Zhu, D. and Miller, R. A. (2002),’Thermal Conductivity and Sintering Behavior of Advanced Thermal Barrier Coatings’, *Ceramic Engineering and Science Proceedings* **23.**

[30] Krupakaran RL, Hariprasad T, Gopalakrishna A (2016) The performance and exhaust emissions investigation of a diesel engine using γ-Al2O3 nanoparticle additives to biodiesel. Carbon Management 7(3–4):233–241

[31] Sachuthananthan B, Krupakaran RL, Balaji G. Exploration on the behaviour pattern of a DI diesel engine using magnesium oxide nano additive with plastic pyrolysis oil as alternate fuel. Int J Ambient Energy 2021;42(6):701–12. https://doi.org/ 10.1080/01430750.2018.1563812.

[32] Dhinesh B, Annamalai M. A study on performance, combustion and emission behaviour of diesel engine powered by novel nano nerium oleander biofuel.J Clean Prod 2018;196:74–83. https://doi.org/10.1016/j.jclepro.2018.06.002.

[33] Krupakaran RL, Gangula VR, Tarigonda H, Sachuthananthan B, Balasubramanian D, Anchupogu P, Petla R, Veerasamy S. The influence of thermal barrier coating (TBC) on diesel engine performance powered by using Mimusops elengi methyl ester with TiO2 nanoadditive. International Journal of Ambient Energy. 2023 Dec 31;44(1):2250-61.

[34] Krupakaran RL, Hariprasasd T, Gopalakrishna A. Experimental investigation on direct injection diesel engine fuelled with addition of titanium dioxide nanoparticle to M. elangi biodiesel for varying injection pressures. Environmental Progress & Sustainable Energy. 2019 Sep;38(5):13207.